EFFECTS OF NONLINEAR AERODYNAMICS AND STATIC AEROELASTICITY ON MISSION PERFORMANCE CALCULATIONS FOR A FIGHTER AIRCRAFT

Gary L. Giles
NASA Langley Research Center
Hampton, VA

Kenneth E. Tatum
Planning Research Corporation
Hampton, VA

Willard E. Foss, Jr.
NASA Langley Research Center
Hampton, VA

INTRODUCTION

During conceptual design studies of advanced aircraft, the usual practice is to use linear theory to calculate the aerodynamic characteristics of candidate rigid (nonflexible) geometric external shapes. Recent developments and improvements in computational methods, especially computational fluid dynamics (CFD), provide significantly improved capability to generate detailed analysis data for the use of all disciplines involved in the evaluation of a proposed aircraft design.

This paper describes a multidisciplinary application of such analysis methods to calculate the effects of nonlinear aerodynamics and static aeroelasticity on the mission performance of a fighter aircraft concept. The aircraft configuration selected for study was defined in a previous study using linear aerodynamics and rigid geometry. The results from the previous study are used as a basis of comparison for the data generated herein. Aerodynamic characteristics are calculated using two different nonlinear theories, potential flow and rotational (Euler) flow. The aerodynamic calculations are performed in an iterative procedure with an equivalent plate structural analysis method to obtain lift and drag data for a flexible (nonrigid) aircraft. These static aeroelastic data are then used in calculating the combat and mission performance characteristics of the aircraft. Comparisons are given between data obtained using conventional methods in the earlier study and the data obtained herein using more rigorous analytical methods.

- **Status**

  Aircraft conceptual design studies based on linear aerodynamic theory and rigid geometric shape

- **Objective**

  To calculate the effects of nonlinear aerodynamics and static aeroelasticity on the mission performance of a fighter aircraft concept

- **Outline**
  - **Configuration definition**
  - **Analytical tools and procedures**
  - **Static aeroelastic results**
  - **Mission performance results**

ARTIST'S CONCEPTION OF TVC AIRCRAFT

This study needed a configuration which would demonstrate the applicability of the methods to realistic geometries, e.g., a complete fighter aircraft. The aircraft chosen needed to provide some complexity without introducing difficulties which would detract from the research goals of the study.

A conceptual drawing of the aircraft selected is shown in the figure. The design incorporates many advanced technologies, including the concept of Thrust-Vector-Control (TVC). The TVC aircraft is a tailless, twin-engine vehicle utilizing multi-axis thrust vectoring for directional control and trim at supersonic speeds, both in cruise (Mach=2.0) and maneuver. The leading- and training-edge devices are intended for subsonic maneuver, take-off and landing.

The configuration is the result of conceptual design studies, and only limited experimental data for the aircraft exist, all for the rigid-body case. Experimental aerodynamic data for both the rigid and deformed shapes would be desirable for comparison with calculated data. The combination of a moderate-to-high wing loading for modern fighters and a relatively thin wing provided the potential for significant aeroelastic effects. Also, the use of thrust vectoring, instead of a horizontal tail, for trim and control eliminated the difficulties of analyzing multiple lifting surfaces, a problem inherent in many current production CFD codes. The simplicity of description coupled with potentially large physical effects made the TVC aircraft a desirable test-bed for the current study.

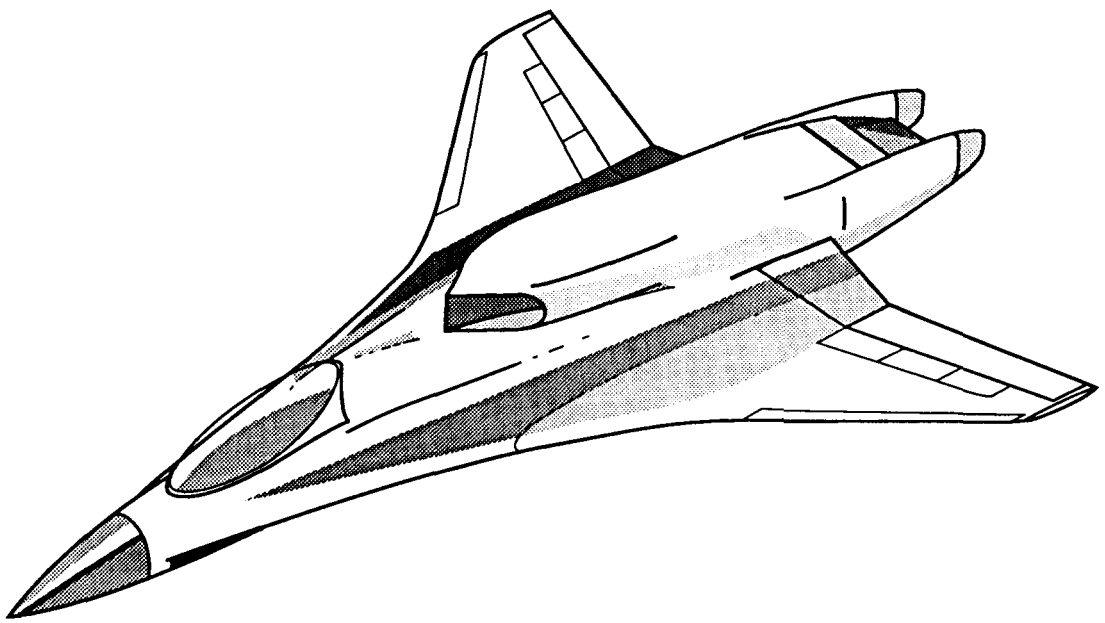

DISCRETIZED MODELS OF THE TVC AIRCRAFT

The TVC aircraft geometry is maintained at NASA Langley in a configuration geometry database which provides a standardized definition of the external geometry as shown at the top of the figure. The fuselage is defined by sets of points which describe the cross-section shapes at specified stations along the length of the fuselage. Lifting surfaces, such as wings, are defined by sets of points which describe airfoil cross sections at specified span locations. In the region of the wing-body intersection, the points on the fuselage are located to provide a smooth transition between the fuselage and wing.

The geometric input data required by the nonlinear aerodynamic analysis programs are illustrated at the bottom of the figure. Geometry data are interpolated from the database geometry at selected cross sections from the nose to the rear of the vehicle. A zero-thickness sheet is defined aft of the wing trailing edge and used for wake calculations. A geometry manipulation program, Ref.1, was used in conjunction with various splining techniques to generate the smooth planar cross-section cuts from the original wireframe definition. The same geometric definition is used for both nonlinear aerodynamic analysis programs used in this study. Note that the inlet geometry could not be represented exactly with the aerodynamic codes used in this study.

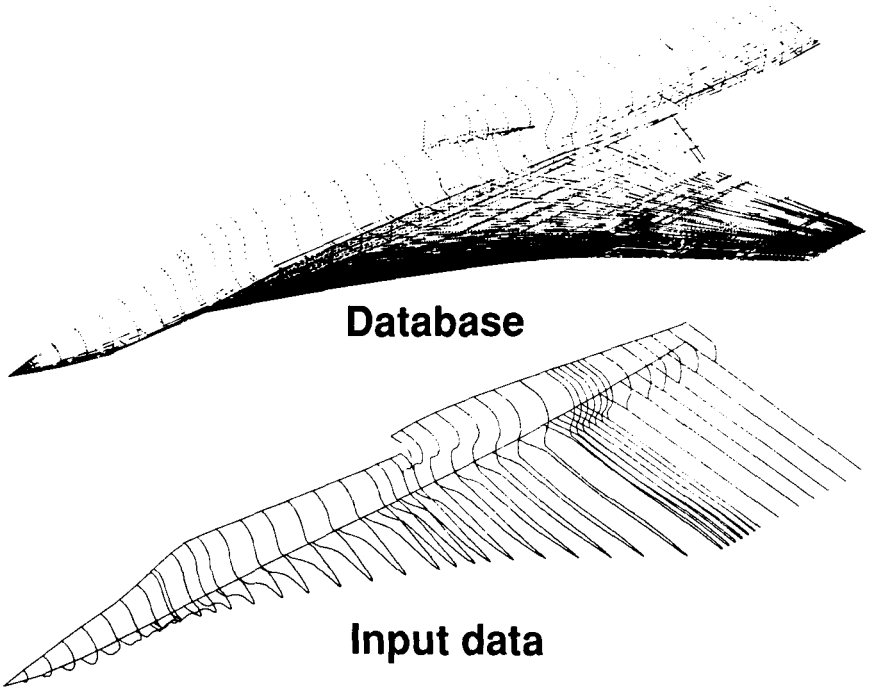

AERODYNAMIC ANALYSIS METHODS

The mission analyses in this study were based on force estimates from three different aerodynamic analysis tools. The baseline mission predictions utilized linear aerodynamic theories with the assumption that the drag is separable into components, e.g. skin friction, wave, etc. (Refs. 2 to 7). Using a "Mach-box" representation of the rigid wing, the induced drag was obtained from linear integral equations and an estimate of attainable leading-edge suction. Far-field wave drag was computed by the supersonic area rule.

In an effort to improve the force predictions, two nonlinear aerodynamic analysis methods were used. The first, SIMP (Ref. 8), solves the conservation-law form of the steady full potential equation by an implicit spatial marching technique. Finite differences are used to discretize the differential equation. The second code, EMTAC (Ref. 9), solves the unsteady Euler equations by a similar spatial marching technique. The discretization is by finite volume flux balancing. Both codes use the same geometry input and grid generation routines. The codes are capable of computing supersonic flow fields for complex geometries, including mass flow into inlets.

The Euler equations include fewer assumptions than the potential equations and, as such, are presumed to be more accurate. However, they also require more computer resources, as would be expected.

- **Linear theory**
  - **Wave drag: supersonic area rule**
  - **Drag-due-to-lift: integral equations**
- **Nonlinear full potential theory (SIMP)**
  - **Finite difference spatial marching**
  - **3D steady inviscid conservation law**
- **Euler theory (EMTAC)**
  - **Finite volume spatial marching**
  - **3D nonlinear inviscid equations**

STRUCTURAL ANALYSIS METHOD

The structural analysis method, Ref. 10, used for this study is implemented in a computer program referred to as ELAPS (Equivalent Laminated Plate Solution). This method requires only a small fraction of the volume of input data compared to a corresponding **finite-element** structural model. The resulting reduction in numerical model preparation is important during early stages of design where many candidate configurations are being assessed. The wing structure is represented as an equivalent plate in this formulation. The planform geometry of the structural box is defined by multiple trapezoidal segments as shown in the figure. A cross-sectional view of a typical segment is also shown. The wing depth, h, camber definition, zc, and cover skin thicknesses, t, are all defined in polynomial form over the planform of a segment.

The Ritz method is used to obtain an approximately stationary solution to the variational condition of the energy of the structure and applied loads. In this method, the wing deflection is assumed to be represented in polynomial form as given for the bending deflection by

$$W = C_{00}+C_{10}x^1+C_{20}x^2+C_{01}y^1+ \ \ldots \ +C_{mn}x^m y^n \qquad (1)$$

The Ritz solution is used to determine the numerical values of the set of unknown coefficients, C_{mn}, which minimize the total energy. The solution, given in the form of Eq.(1), provides a continuous functional definition of the wing deflection over the planform. This continuous definition expedites the interface of the structural and aerodynamic calculations.

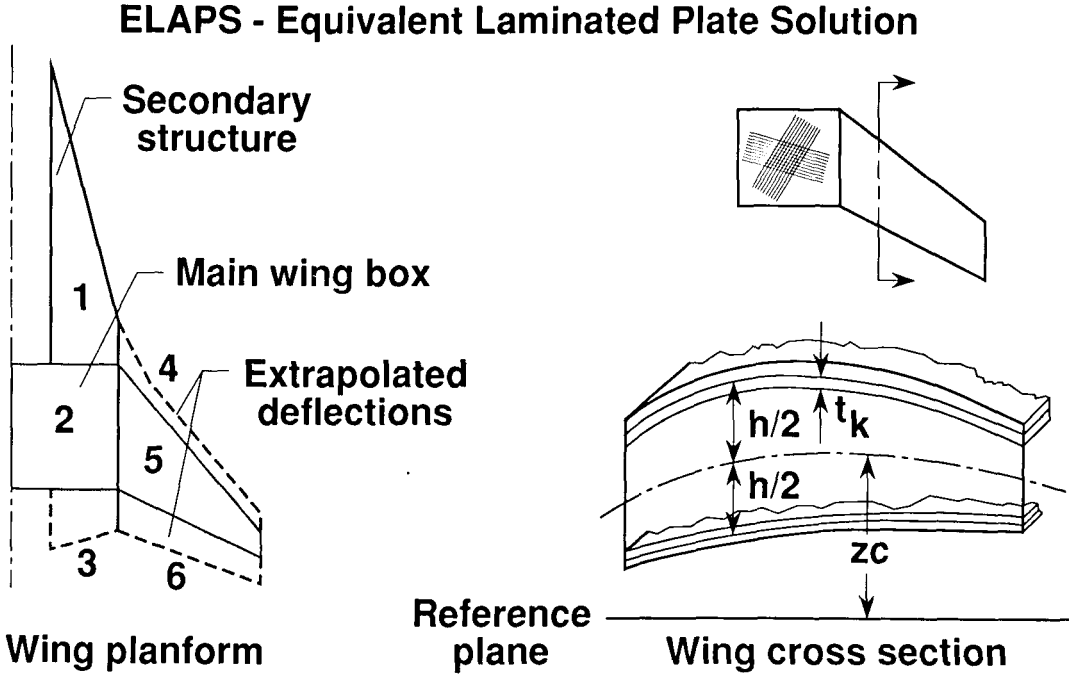

MISSION ANALYSIS METHOD

A computer program which calculates the mission radius and maneuverability characteristics of combat aircraft, Ref. 11, is used in this study. This program has been used at the Langley Research Center to assess mission performance of proposed configurations and to indicate associated research programs which would be expected to yield the most beneficial improvements, Ref. 12. The program can be used (1) in an analysis mode to determine the performance characteristics of a given configuration or (2) in a sizing mode to determine the configuration size in terms of takeoff gross weight, wing loading, and thrust-to-weight ratio that best meets all the mission performance constraints. Only the analysis mode is used in this study.

A variety of military missions can be specified by using a desired combination of modules to calculate performance data for take-off, climb, cruise, loiter, dash, combat, descent, reserves, and landing segments of a mission profile. The definition of the aircraft is given in terms of propulsion system characteristics, aerodynamic characteristics, along with size and weight of the vehicle. The propulsion characteristics are precomputed, usually from data supplied by an engine manufacturer. The aerodynamic characteristics are represented in terms of lift and drag coefficients as functions of aircraft angle of attack and flight Mach number. The size of the aircraft is defined in terms of the wing area, the size and number of engines, and the take-off gross weight.

- **Program used at Langley Research Center to calculate mission radius and maneuverability characteristics of military aircraft**
- **Flight segments used**

Takeoff	Climb	Cruise
Loiter	Dash	Combat
Descent	Reserves	Landing

- **Inputs to program**
  - **Propulsion (engine decks)**
  - **Aerodynamics (C_L and C_D vs. α and M)**
  - **Aircraft size (wing area, takeoff gross weight)**

COMPUTING ENVIRONMENT

This study is typical of multidisciplinary analysis/design efforts in that several existing computer programs are used with each program being operated by a disciplinary specialist. The computer programs used in this study resided on several different computers as indicated on the figure. No attempt was made to convert all programs to reside on a single machine. Instead, procedures were set up to accommodate communication of data between the various machines and programs. The required interfaces between the programs were written so as to minimize the volume of data that was transmitted between computers.

The size and location of the computers used included a MicroVAX II on an engineer's desktop, the CYBER 800 series computers at the NASA Langley central computer site, and the more powerful CYBER 205 and CRAY 2 required by the nonlinear aerodynamic programs. The CRAY 2 is part of the NAS computer complex located at NASA-Ames.

Computer program	Computer	Operating system
GEOM	CYBER 800 series	NOS
Middleton-Carlson	CYBER 800 series	NOS
Harris wave drag	CYBER 800 series	NOS
SIMP	CYBER 205	VSOS
EMTAC	CRAY 2	UNICOS
ELAPS	MicroVAX II	VMS
Mission analysis	CYBER 800 series	NOS

TVC MISSION DEFINITION

The primary mission for the TVC is one of high-altitude interdiction. The aircraft was designed to cruise at Mach 2 with a radius of 500 nautical miles. A payload of 2900 lbs. is expended at the radius station. Combat requirements are for one and a half sustained turns at Mach 2 at an altitude of 40,000 ft. with an ultimate maneuver criteria of 8.1 g load factor. The mission performance calculations used the following fuel allowances. The takeoff fuel allowance is taken to be the fuel required to operate the engines for one-half minute at the maximum augmented thrust level and then for one minute at the maximum non-augmented thrust level. Fuel allowance for combat is the amount required to meet the combat requirements given above. The reserve fuel allowance is the fuel required to loiter for 20 minutes at sea level.

The majority of the mission is performed with the aircraft at Mach 2 cruising conditions (outbound and inbound). Combat conditions occur for a small percentage of time. The relative time spent in each of these conditions has a considerable impact on the performance results presented later.

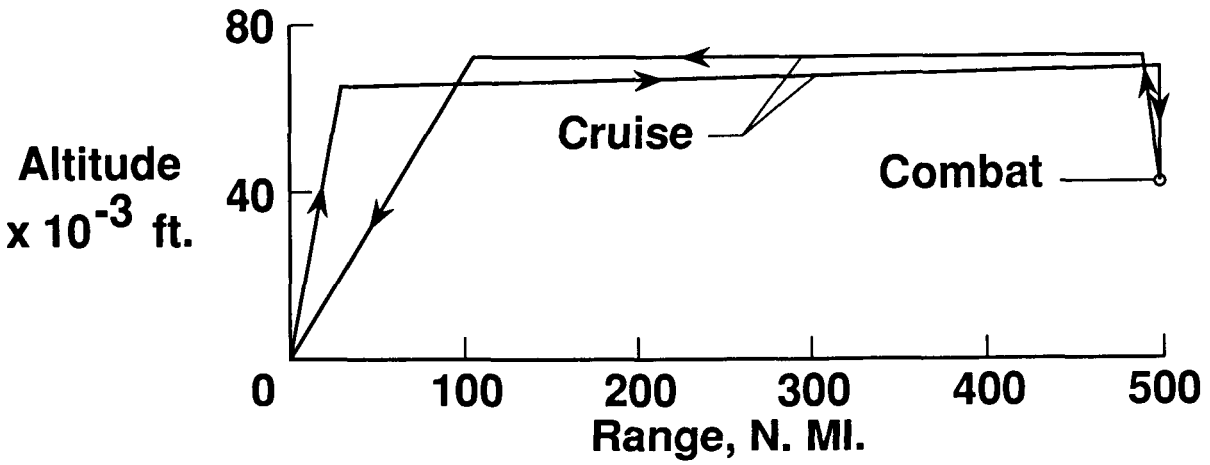

- Cruise Mach number = 2.0
- Payload = 2900 lbs; expended at radius station
- Combat is for 1 1/2 turns at max. sustained turn rate at Mach number = 2.0 and altitude = 40 000 ft

FLEXIBLE WING AERO/STRUCTURAL ANALYSIS PROCEDURE

A flow chart of the iterative procedure to arrive at the aeroelastically deformed shape of a wing at a specified flight condition is shown in the figure. A detailed discussion of the original development of this procedure is given in reference 13. The process is initiated with the geometric shape determined during the conceptual design studies taken to be the shape of the flexible aircraft at cruise. This baseline shape is analyzed at cruise to yield the jig (fabrication) shape, and at maneuver for an initial estimate of the elastic maneuver loads. Application of these maneuver loads to the jig shape produces an initial approximation to to the elastic maneuver shape. Iteration proceeds by computing loads on the current maneuver shape approximation and applying these loads to the jig shape. At each aerodynamic load analysis the maneuver lift is maintained by adjusting the aircraft angle of attack. Convergence is achieved when the calculated air loads are consistent with the structural deflection from the jig shape. The converged aerodynamic characteristics are then used in mission analysis calculations.

The continuous definition of the deformed wing shape used in ELAPS expedites the interface between the aerodynamics and structures programs. An equivalent load vector corresponding to the number of unknown displacement function coefficients, Eq. 1, is required for analysis of the equivalent plate structure. This load vector is formed by integrating the product of the aerodynamic pressure and displacement function terms over each portion of the aerodynamic grid on the wing surface. In the structures-to-aero interface, these continuous, analytic definitions of displacements are evaluated at each point of the aerodynamic input geometry and used directly to generate a deformed configuration.

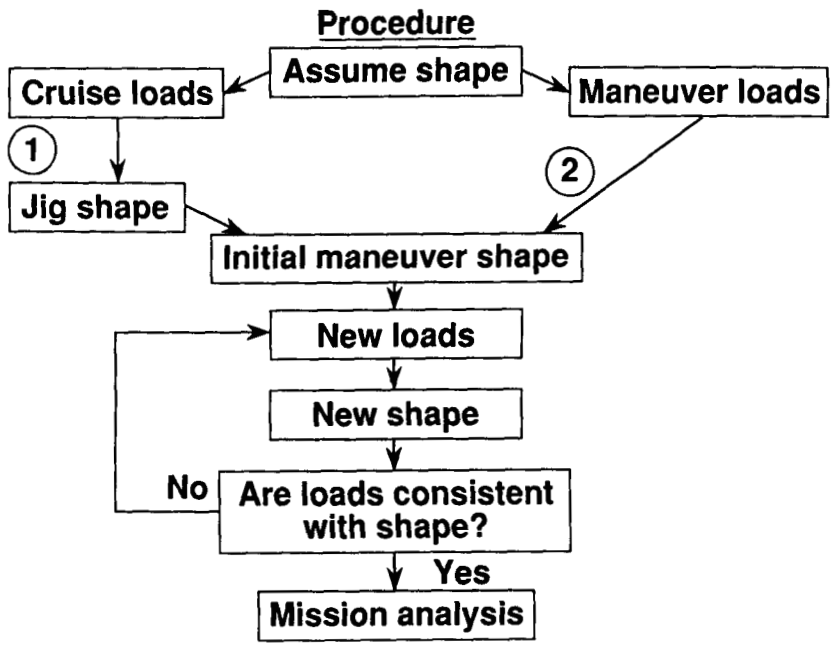

CONVERGED STRUCTURAL DISPLACEMENTS

During this design study, the thickness distribution of the wing cover skins was sized initially using loads on the rigid cruise shape at the 8.1g load factor. The deflection, calculated in the aeroelastic analysis, of this first structural model, herein referred to as wing 1, caused an inboard shift of the aerodynamic pressures and a corresponding reduction in stress levels in the cover skins. The thickness of the wing skins was then resized using the 8.1g aeroelastic loads. This wing with resized (reduced thickness) skins is referred to as wing 2.

A reduction in aircraft weight, as a result of going from wing 1 to wing 2, is not included in subsequent performance calculations. The aircraft weight was estimated using weight equations which inherently include the effect of reduced structural loads resulting from aeroelastic deformation.

The converged structural deformations at 8.1g load factor for wing 2 as computed by SIMP/ELAPS are shown in the figure. The maximum deflection (measured from the baseline cruise geometry) was 20.01 inches at the wing tip trailing edge. The loading caused the wing to twist 6.08 degrees, leading edge down. Similar results were obtained by EMTAC/ELAPS with the maximum deflection increasing to 21.37 inches.

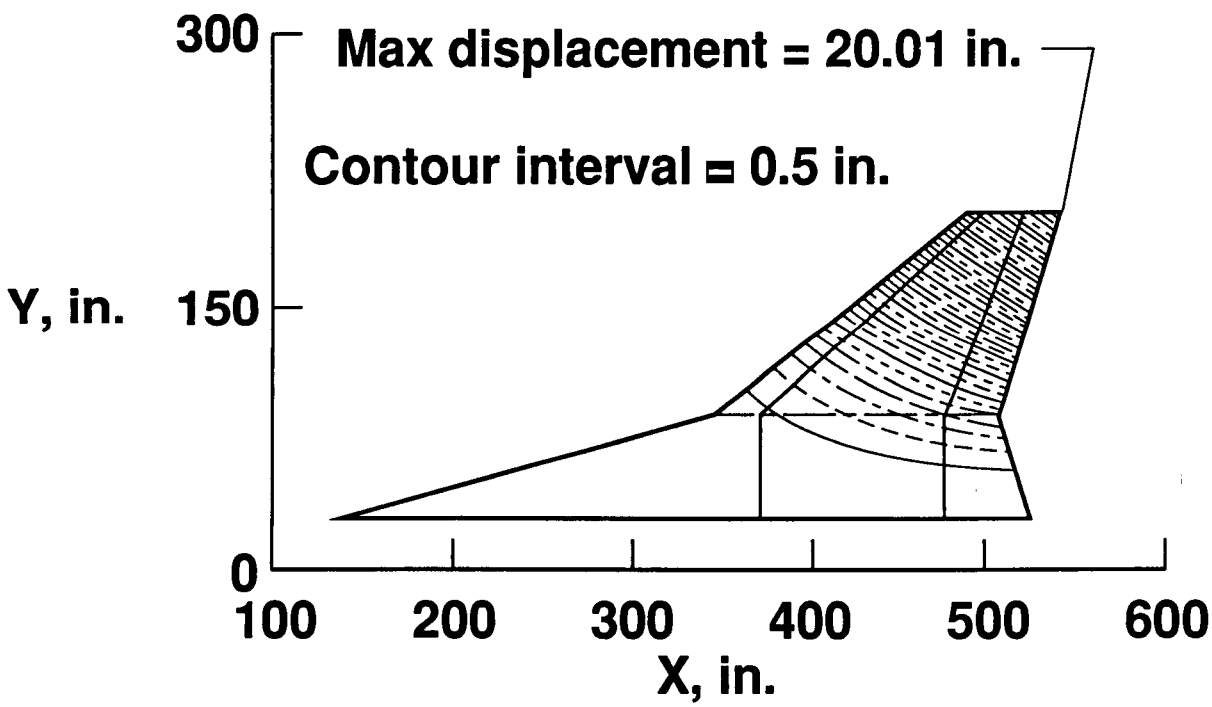

AERODYNAMIC CROSS-PLANE GRID

The level of detail of the analytical representation used in the solution of the aerodynamic flow equations is illustrated in this figure. A representative cross-plane grid at a specific body station is shown for one of the deformed wing geometries computed by SIMP. Both SIMP and EMTAC employ streamwise marching schemes to integrate the flow equations on successive planes, such as the one shown. A conical flow similarity solution is generated to start the calculation on a plane near the nose of the aircraft, which is assumed to be sharp, thereby allowing an attached bow shock wave. This starting solution defines the incoming flow for the next plane a small step downstream. By repetitively stepping (marching) from one plane to the next, the entire length of the body is traversed. On each plane a two-dimensional grid is constructed about the body cross-section, as shown, and a numerical difference approximation to the flow equations is solved for the dependent variables(s), which for EMTAC are the density, velocity components, and internal energy. Pressure can then be directly computed from these quantities using the ideal gas law. In SIMP the velocity components are computed by numerically differentiating the velocity potential. Pressure and density are then computed by the ideal gas law and the Bernoulli equation. Thus, at each longitudinal station down the body **surface, the flow variables, such as pressure, are computed at discrete** locations on the body surface and off the surface in the flow field.

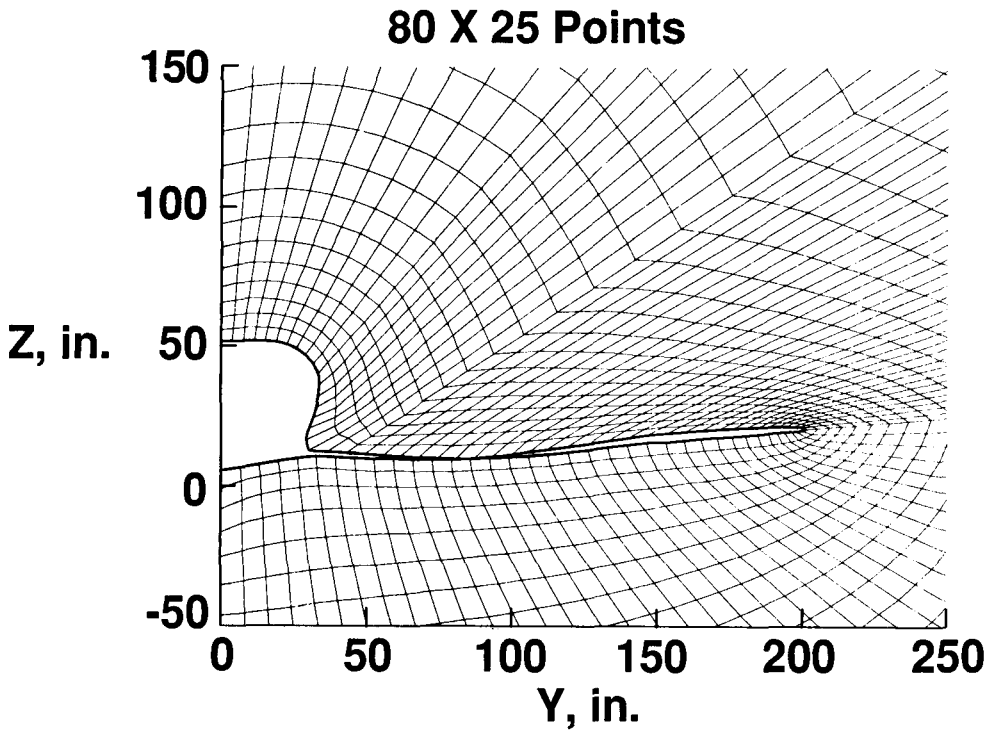

DETAILS OF THE AERODYNAMIC FLOW FIELDS

By using grids such as the one shown in the previous figure, the nonlinear aerodynamic codes provide a high degree of resolution of the flow fields about the aircraft. The contour plots of cross-plane pressure shown in this figure are representative of the detail attainable with SIMP and EMTAC. Such plots allow the calculated loads/pressures to be interpreted in light of the physics being modeled by the differential equations. For example, an upper-surface cross-flow shock wave is predicted by SIMP, evident in the concentration of isobars near Y=100. However, EMTAC does not indicate a shock impinging on the wing. Such localized differences in the flow field contribute to differences in the overall load distributions and resulting deflections in the aeroelastic calculations. While each aerodynamic code gave substantially different computed flow features (i.e. shocks, expansions, etc.), the overall character of each of these flow fields did not change significantly during the aeroelastic iterations with a given aerodynamics code. Even at the high maneuver conditions (8.1g's) where large structural deflections were computed, the overall character of the flow fields did not change, however the relative magnitudes or strengths of the aerodynamic pressures were affected by the deflections.

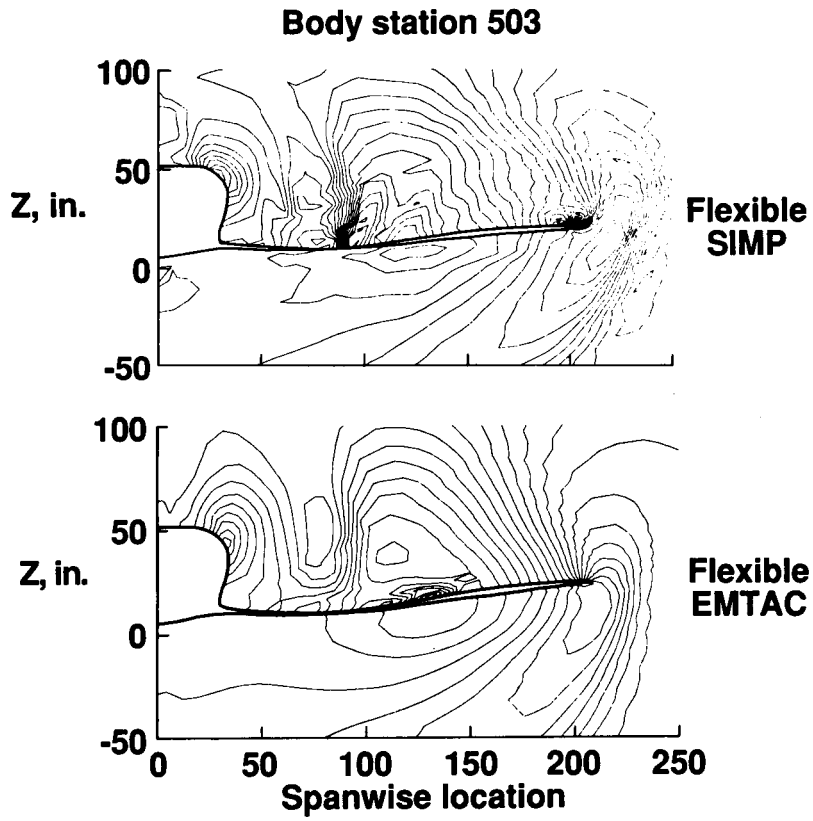

COMPARISON OF SPANWISE PRESSURE DISTRIBUTIONS

The aerodynamics and structural analysis codes were coupled through the aerodynamic loads as represented by pressure coefficient distributions over the wing surface. Representative spanwise pressure variations are shown in this figure as computed by SIMP and EMTAC at specific axial (body) stations. Two of these distributions are for the baseline rigid geometry while the third is for the aeroelastically deformed solution as computed by EMTAC/ELAPS. Each plot is part of the overall solution at a vehicle lift coefficient of approximately 0.361, however the section lift coefficient at each body station changes due to axial shifts of the load distribution produced by different aerodynamic theories and from the aeroelastic deformations.

A significant feature of these distributions is the unloading of the outboard wing region due to the static aeroelastic deformation. Also significant is the more physically realistic loading computed by EMTAC as opposed to SIMP in the region of the wing tip. At the high lift conditions required for **maneuver, the assumption of potential theory is questionable,** and, while this study has shown usable results from a potential flow code, indications are that the more complete theory, represented by the Euler equations, provides more reliable results.

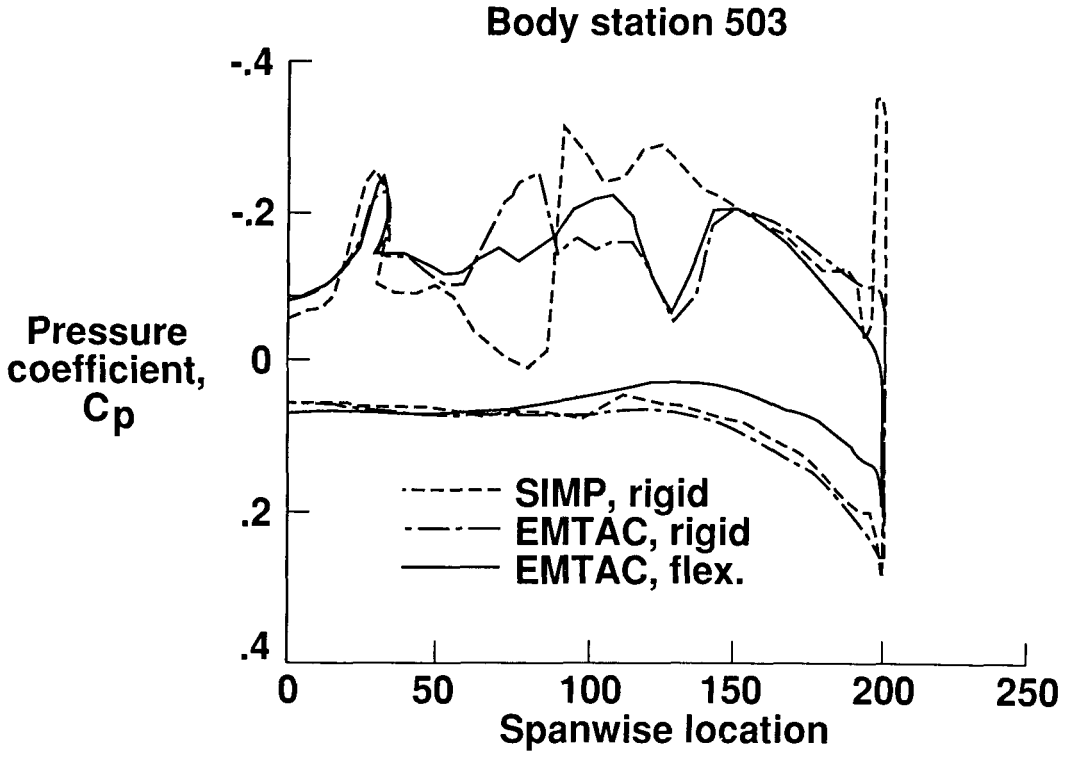

FORCE PREDICTIONS FOR THE TVC AIRCRAFT

As the pressure distributions are key quantities in the static aeroelastic computations, the integrated pressures in the forms of drag and lift are key quantities in performance calculations. The solid curve shown in the figure is the drag polar computed by the baseline linear aerodynamic theory, including the induced drag (often referred to as drag-due-to-lift) and the wave drag, assumed to be a constant at a given Mach number. Selected nonlinear aerodynamic calculations are shown by the symbols for both rigid and flexible geometries. At low lift coefficients, the difference in results between nonlinear aerodynamic theories, including the effects of static aeroelasticity, is negligible and single symbols are shown to indicate the drag increment predicted by nonlinear theory. At higher lifts, however, the differences are noticeable with progressively higher drag predicted by SIMP and EMTAC, with rigid and flexible geometries. In particular, for the case of a flexible wing, the drag coefficient from aeroelastic calculations using EMTAC (Euler theory) is about 0.0025 greater than that calculated using SIMP (Full potential theory).

Note that while the linear theory assumes separable wave and induced drag, the nonlinear theories include both of these components in the calculation of a single drag value.

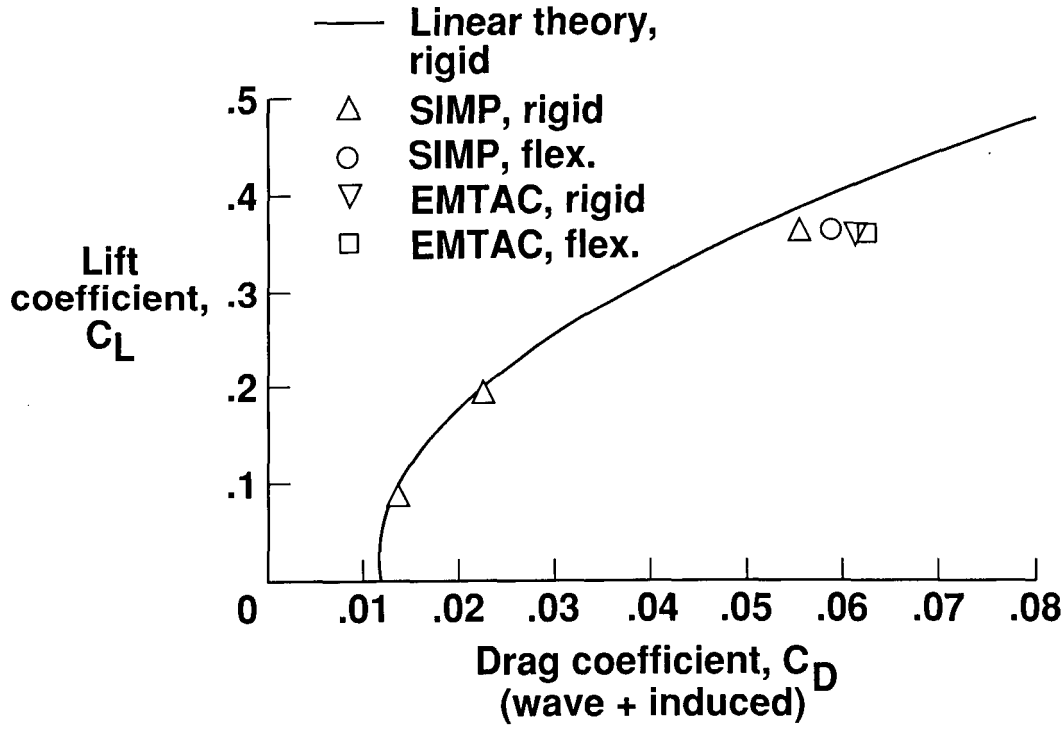

AERODYNAMIC DATA FOR PERFORMANCE ANALYSIS

The required aerodynamic input to the mission analysis program consists of the lift, drag, and angle of attack variations for the specified mission. These three variables are related as shown in the figure for the baseline linear theory prediction and the SIMP and EMTAC predictions for the rigid and flexible geometries. The angle of attack is an input to SIMP and EMTAC and the C_L is computed from the integrated pressures. The C_D shown includes the estimated skin friction and roughness drag. These latter two components were identical to those used in the original linear theory calculations. An analysis code solving the Navier-Stokes (viscous) equations would couple these effects with the wave and induced drag components and eliminate this approximation.

The curves shown for the nonlinear rigid/flexible cases were derived by curve fitting the values obtained from a limited set of computations since this was a research project, not an aircraft development project. Basic assumptions for the curve-fits were: 1.) the nonlinear predictions converged to the same values at low lift, and 2.) both the C_L/alpha and C_L/C_D curves were of second order. As might be expected, the linear predictions are the most optimistic **and include nonlinear theory and/or static aeroelasticity** results in degradation of the available lift and increase in predicted drag.

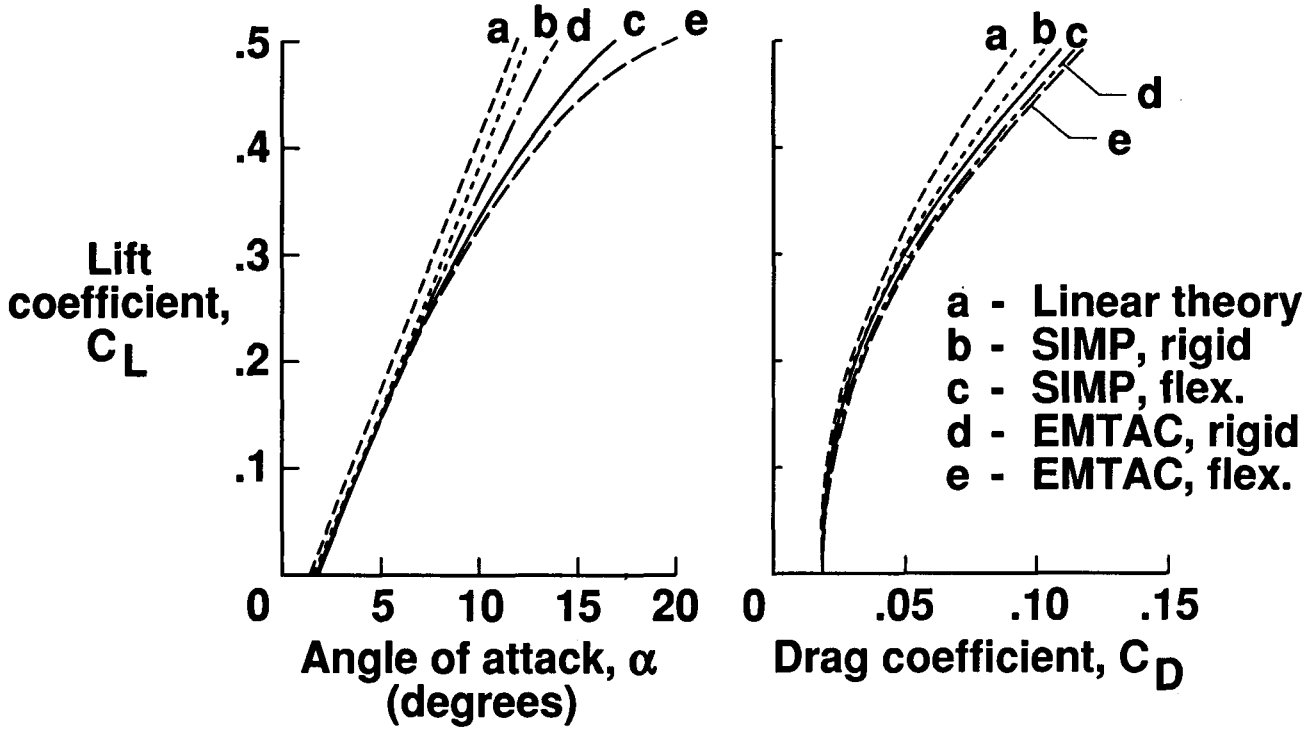

COMBAT PERFORMANCE OF THE TVC AIRCRAFT

The effect of nonlinear aerodynamics and static aeroelasticity on the combat performance of the TVC aircraft is indicated on the figure. The specific power, P_s, is a measure of the energy maneuverability of an aircraft for combat. This parameter is a direct function of the difference between the thrust and the drag. The load factor for maximum sustained turning occurs where the specific power is equal to zero. At a greater load factor, the specific power is negative and the aircraft is not able to sustain the flight condition. The increased drag levels of the nonlinear aerodynamic and the non-rigid structural considerations result in lower sustained load factors and associated turn rates. The decrease in load factor is from a value of 8.1g's to about 7.1g's. In addition to the loss in maneuvering capability, the amount of fuel used during combat is increased from 1000 lbs. to 1143 lbs. Consequently, the fuel available to cruise is reduced and as a result the mission radius capability is reduced.

As indicated, using the different nonlinear aerodynamic theories result in the largest reduction in calculated combat performance, with aeroelasticity contributing a somewhat smaller increment. Consideration of aeroelasticity often has a significant effect on maximum roll rate characteristics of a fighter aircraft, Refs. 14 and 15. However, the roll rate characteristics of the TVC aircraft were not calculated in this study.

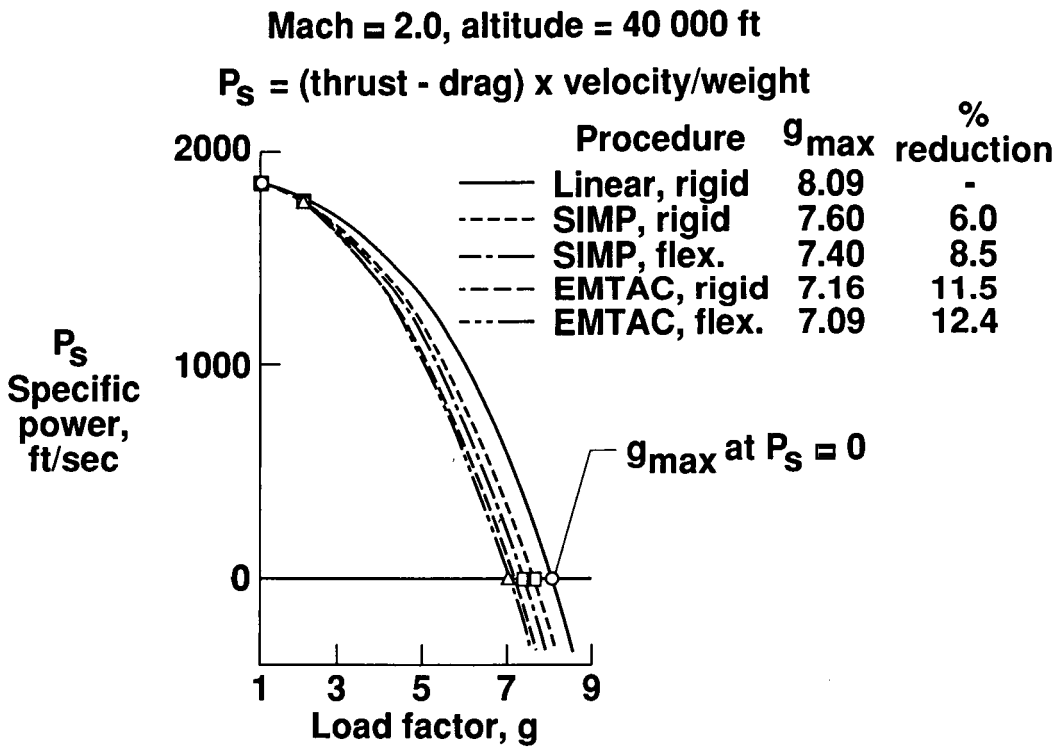

MISSION PERFORMANCE OF THE TVC AIRCRAFT

The increased drag levels estimated for the nonlinear aerodynamics and for the flexible structural considerations result in mission radius losses of up to 68 N.Mi. Approximately 75 percent of each of the losses is due to the reduced cruise efficiency as a direct result to the increased drag estimates given by the nonlinear codes. The remaining 25 percent of each of the losses is due to the reduction in available cruise fuel associated with the increased combat fuel allowance.

As would be expected for this particular mission, the effect of aeroelasticity on aircraft range is minimal. However, for a mission in which a large percentage of total time is spent in combat conditions, including the effects of aeroelasticity in design and analysis could become important.

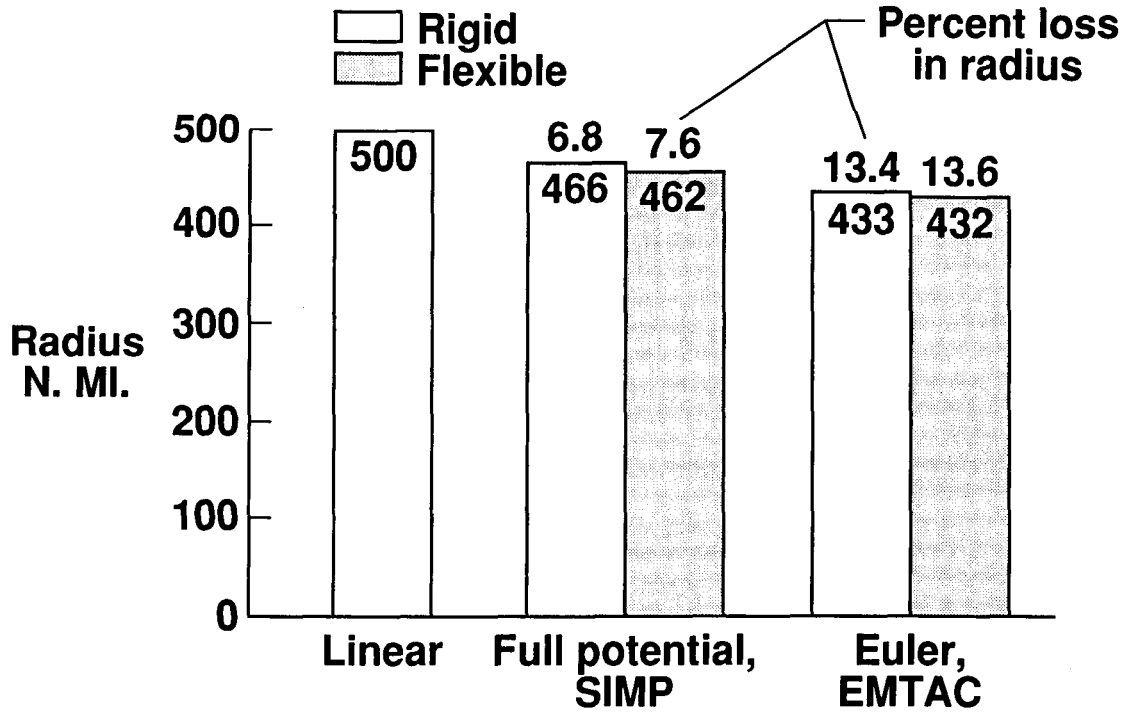

CONCLUDING REMARKS

A multidisciplinary analysis procedure has been developed that includes aerodynamic, structural and performance calculations. Use of this procedure is demonstrated by analyzing the effects of nonlinear aerodynamics and static aeroelasticity on the performance of a TVC fighter aircraft. Representation of the wing structure as an equivalent plate allows aeroelasticity considerations to be included early in the design process before a finite element model is available. In addition, the continuous definition of the wing deformation permits the interface to the aerodynamics programs to be written in a simple but general manner. Two programs, one based on full potential theory and the other based on Euler theory, were incorporated to provide a comparison of the effect on the calculated aerodynamic characteristics. There were significant differences in the pressure fields and the Euler theory predicted higher overall drag than full potential theory.

The aircraft performance was affected primarily by aerodynamic theory rather than aeroelastic effects. The combined effect gave a maximum loss in sustained load factor of 12% and a mission radius loss of 14% compared with linear aerodynamic calculations on a rigid aircraft. The cost-effectiveness of using these more rigorous analytical procedures for preliminary design must be determined by individual design organizations. As is demonstrated, this procedure provides the capability to provide refined design data. However, the potential for these data to provide improvements in the final aircraft design must be assessed in view of the practical limitations imposed by budget and calendar time for a particular project

- **Multidisciplinary analysis procedure developed that includes aerodynamic, structural, and performance calculations**
- **Equivalent plate structural representation expedites aeroelastic calculations**
- **Significant differences in pressure fields with improvements in aerodynamic modeling (linear, full potential, Euler)**
- **Performance affected primarily by aerodynamic theory; maximum sustained load factor loss ≅ 12% mission radius loss = 14%**
- **Cost-effectiveness of procedure decided by user**

REFERENCES

1. Hall, J. F.; Neuhart, D. H.; and Walkley, K. B.: An Interactive Graphics Program for Manipulation and Display of Panel Method Geometry. NASA CR 166098, March 1983.

2. Sommer, S. C.; and Short, B. J.: Free-Flight Measurements of Turbulent-Boundary-Layer Skin Friction in the Presence of Severe Aerodynamic Heating at Mach Numbers from 2.8 to 7.0. NACA TN 3391, 1955.

3. Harris, R. V., Jr.: An Analysis and Correlation of Aircraft Wave Drag. NASA TM X-947, 1964.

4. Carlson, H. W.; and Middleton, W. D.: A Numerical Method for the Design of Camber Surfaces of Supersonic Wings With Arbitrary Planforms. NASA TN D-2341, 1964.

5. Sorrells, R. B.; and Miller, D. S.: Numerical Method for Design of Minimum-Drag Supersonic Wing Camber With Constraints on Pitching Moment and Surface Deformation. NASA TN D-7097, 1972.

6. Carlson, H. W.; and Miller, D. S.: Numerical Methods for the Design and Analysis of Wings at Supersonic Speeds. NASA TN D-7713, 1974.

7. Middleton, W. D.; and Lundry, J. L.: A System for Aerodynamic Design and Analysis of Supersonic Aircraft. NASA CR 3351-3354, 1980.

8. Shankar, V.; Szema, K-Y; and Bonner, E.: Full Potential Methods for Analysis/Design of Complex Aerospace Configurations. NASA CR 3982, May 1986.

9. Szema, K-Y; Chakravarthy, S.; and Shankar, V.: Supersonic Flow Computations Over Aerospace Configurations Using an Euler Marching Solver. NASA CR 4085, July 1987.

10. Giles, G. L.: Further Generalization of an Equivalent Plate Representation for Aircraft Structural Analysis. NASA TM 89105, February 1987.

11. Foss, W. E., Jr.: A Computer Technique for Detailed Analysis of Mission Radius and Maneuverability Characteristics of Fighter Aircraft. NASA TP 1837, March 1981.

12. Coen, P. G.; and Foss, W. E., Jr.: Computer Sizing of Fighter Aircraft. NASA TM 86351, January 1985.

13. Tatum, K. E.; and Giles, G. L.: Integrating Nonlinear Aerodynamic and Structural Analysis for a Fighter Configuration. AIAA Paper No. 87-2863. Presented at the 1987 AIAA/AHS/ASEE Aircraft Design, Systems and Operations Meeting, St. Louis, Missouri, Sept. 14-16, 1987.

14. Static Aeroelasticity in Combat Aircraft. AGARD Report No. 725, January 1986.

15. Static Aeroelastic Effects on High Performance Aircraft. AGARD Conference Proceedings No. 403, July 1987.